Escherichia coli Transcription Termination Factor Rho Binds and Hydrolyzes ATP Using a Single Class of Three Sites†

Barbara L. Stitt*

Department of Biochemistry and Fels Institute for Cancer Research and Molecular Biology, 3420 N. Broad Street, Philadelphia, Pennsylvania 19140

Received September 25, 2000; Revised Manuscript Received December 11, 2000

ABSTRACT: *Escherichia coli* transcription termination factor Rho uses the energy of ATP hydrolysis to travel 5′ → 3′ along RNA. We previously showed that the hexameric Rho protein binds three molecules of ATP in active sites and that hydrolysis of the three bound ATP molecules upon RNA binding is sequential. Other models of Rho ATP hydrolysis activity have arisen from reports of additional ATP binding sites on Rho. Here we present further evidence from binding, isotope partitioning, and rapid mix/chemical quench experiments, in support of the presence of only three equivalent ATP binding sites on Rho that are catalytic sites and that fire sequentially. These results are incorporated into a proposed mechanism for directional Rho tracking along RNA.

Escherichia coli transcription termination protein Rho aids in the release of newly synthesized RNA from paused transcription complexes (reviewed in ref *1*). The homohexameric Rho protein binds nascent RNA and, with the RNA-dependent hydrolysis of ATP, disrupts the ternary transcription complex, releasing product RNA and allowing RNA polymerase to recycle. An ATP-dependent RNA−DNA helicase activity of Rho is thought to be important to its function in transcript release (*2*, *3*).

No high-resolution three-dimensional structure is available for the Rho hexamer; however, electron microscopy and cross-linking studies indicate a toroidal C_3 arrangement of subunits (*4*, *5*), reminiscent of several other homohexameric helicases, such as the T7 gene 4 product (*6*), with which Rho shares limited amino acid sequence similarity only in the presumptive NTP binding region (*7*). X-ray crystallography and NMR-derived three-dimensional structures have been obtained for the N-terminal 130 (of 419) amino acids of Rho, which comprise the RNA-binding domain (*8*−*10*).

The protein most similar to Rho in amino acid sequence is mitochondrial F_1 ATP synthase, with 26% identity and 58% similarity (*11*−*13*). Although F_1 has an $\alpha_3\beta_3$ rather than an α_6 composition, the α and β subunits are similar to one another in amino acid sequence and in protein folding (*14*). While the RNA-binding N-terminal portion of Rho is unlike F_1, the amino acid sequence similarities between the ATP-binding portions of these two proteins have stimulated modeling of Rho according to the F_1 structure (*13*, *15*−*17*).

Rho and F_1 are similar in several additional respects. Functionally, F_1 is a trimer, with three rapidly exchanging, catalytic adenine nucleotide binding sites that operate sequentially in overall catalysis (*14*). These features are also present in Rho. ATP and RNA binding data and hexamer assembly experiments support the conclusion that Rho behaves as a trimer of dimers (*18*−*21*). Three ATP binding sites that are catalytic sites have been demonstrated in binding and isotope partitioning experiments (*18*). Rapid mix/chemical quench experiments (*22*) indicated that when RNA binds a complex of Rho with three ATP molecules (Rho·ATP_3), hydrolysis of the three bound ATP molecules is sequential. The similarities of functionally trimeric structure and ATP hydrolysis patterns between Rho and F_1 are striking.

An additional common feature between Rho and F_1 is the unusual property of catalytic site cooperativity, in which events in one active site affect the rate of catalysis in other active sites of the multimer (*14*). In the case of ATP hydrolysis by F_1, substrate binding in a second active site greatly enhances the rate of product release from the first site (*14*). For Rho, the rate at which chemistry occurs is affected: RNA-dependent ATP hydrolysis is 30-fold slower when a single ATP molecule is bound to the hexamer than when all ATPase sites are filled (*22*).

The documented structural and functional similarities between Rho and F_1 have prompted searches for additional common properties. One feature of F_1 is the presence of three adenine nucleotide binding sites that are not catalytic and in which exchange of bound nucleotide with free nucleotide is slow compared to the three rapidly exchanging catalytic sites (*14*). Initial studies of ATP binding to Rho documented only three identical sites per hexamer, $K_D = 0.2$ μM (*18*). Subsequent experiments (*19*) confirmed the presence of three ATP binding sites with $K_D = 0.3$ μM, but also reported one to three additional sites of 10-fold lower affinity. However, in later experiments only a single class of three sites on Rho was found (*22*, *23*). Nevertheless, Kim et al. (*23*) and Kim and Patel (*24*) have proposed the existence of ATP binding sites in addition to the three catalytic sites on Rho. In their model, Rho has three higher affinity "noncatalytic" sites in which on-enzyme ATP hydrolysis takes place at 2 s^{-1}, and three lower affinity catalytic sites that turn over at 30 s^{-1}.

† This work was supported by NIH Grant GM60247.

* To whom correspondence should be addressed. Phone: (215) 707-8152. E-mail: stitt@unix.temple.edu. Fax: (215) 707-7536.

10.1021/bi002253a CCC: $20.00
Published on Web 01/19/2001

Measurement by these workers of product ADP off-rates from Rho by nitrocellulose filter-binding suggested that when the Rho catalytic sites were rapidly hydrolyzing ATP, product ADP release from the noncatalytic sites was at only 0.02 s^{-1}. When ATP was depleted, the latter off-rate increased. This model is of considerable interest in that it would constitute another similarity between Rho and F_1; however, it challenges previous data (*22*).

We present the results of additional binding and chemical quench/isotope partitioning experiments to clarify the number and nature of ATP binding sites on Rho and the hydrolysis rates of bound ATP molecules. Equilibrium binding results reconfirm the presence of only a single class of three high-affinity ATP binding sites. When these sites are occupied by [γ-^{32}P]ATP and the complex is mixed with RNA plus nonradioactive ATP, a burst of hydrolysis of one molecule of [γ-^{32}P] ATP is seen at the earliest measurement time, followed by the sequential hydrolysis of the remaining bound [γ-^{32}P]ATP molecules, each at the rate of 30 s^{-1} at 21 °C. Furthermore, when Rho containing three bound nonradioactive ATP molecules is mixed with RNA plus free [γ-^{32}P]-ATP, hydrolysis of the [γ-^{32}P]ATP occurs only after a lag of about 100 ms. These experiments provide evidence to support a model in which, upon RNA binding to Rho·ATP_3, each of the three catalytic sites in turn hydrolyzes its bound ATP molecule, releases products, and binds a new ATP molecule. The first of the three newly bound ATP molecules is then hydrolyzed, beginning a second cycle of hydrolysis around the hexamer.

MATERIALS AND METHODS

Enzymes, Substrates, and Buffers. Wild-type Rho from *E. coli* was purified as described (*25*) from strain AR120/A6 containing plasmid p39ASE (*26*). The concentration of Rho was spectrophotometrically determined using $\epsilon^{1\%}_{280nm} = 3.25$ cm^{-1} (*27*). The enzyme preparation used had a specific activity with poly(C) at 37 °C of 10 units mg^{-1}. A unit of activity is defined as that amount of enzyme that hydrolyzes 1 μmol of ATP in 1 min.

[γ-^{32}P]ATP at a specific activity of 1−10 Ci $mmol^{-1}$ was synthesized from [^{32}Pi] and ATP according to the exchange method of Glynn and Chappell (*28*) as modified by Grubmeyer and Penefsky (*29*). Following purification, this preparation typically had less than 3% of its radioactivity in compounds other than ATP. 1,N^6-etheno-adenosine 5′-triphosphate (ϵATP)[1] from Molecular Probes (Eugene, OR) was similarly radiolabeled in the gamma position. [2,8-^{3}H]-ATP, 10−30 Ci $mmol^{-1}$, catalog no. MT619, was from Moravek Biochemicals, Brea, CA. [2,8-^{3}H]ADP, 25−40 Ci $mmol^{-1}$, catalog no. NET241, and [α-^{32}P]ATP, 800 Ci $mmol^{-1}$, catalog no. BLU003X, were from New England Nuclear.

Poly(C) with an average length of 400 bases was from Amersham Pharmacia Biotech and was dissolved in water at 5 mg/mL.

Buffers were TKME [40 mM Tris-HCl, pH 7.7, at 25 °C, 50 or 100 mM KCl (no differences were found between experiments carried out under the two KCl concentrations), 1 mM $MgCl_2$, and 0.1 mM EDTA] and TAGME (40 mM Tris-acetate, pH 8.3, at 25 °C, 150 mM potassium glutamate, 1 mM magnesium acetate, and 0.1 mM EDTA). Buffers were supplemented with $MgCl_2$ or magnesium acetate at a concentration equimolar with that of any added ATP.

Binding Measurements. Centrifuge columns were used as described by Penefsky (*30*). Briefly, 1 mL columns of G50 (fine) Sephadex (Amersham Pharmacia Biotech) in 1 mL disposable tuberculin syringes were preequilibrated with the desired buffer and centrifuged at 900*g* for 2 min in a swinging bucket rotor. Following the application of 100−200 μL of sample, the column was centrifuged identically a second time, and the eluate was analyzed. All steps were carried out at 21 °C. (1) Approximately 3 pmol of [^{3}H]ATP (200 000 cpm) was mixed with 100 μL of Rho solution at 1 mg/mL (0.35 nmol of hexamer) in TKME buffer. A sample (100 μL) of this mixture was mixed by rapid pipetting with an equal volume containing 20 μg of poly(C) (0.6 nmol of 100-base-long regions) plus 20 mM unlabeled MgATP in the same buffer and was immediately loaded onto a centrifuge column and centrifuged. Less than 20 s elapsed between the start of mixing of the two solutions and the start of separation in the centrifuge. The column eluate was sampled for radioactivity. (2) For detection of [^{3}H]ADP binding to Rho under hydrolysis or mock hydrolysis conditions, mixtures were made in TKME buffer that were 1.5 μM Rho hexamer; 80−320 μM [^{3}H]ADP at 9000 cpm/nmol; 0.033, 1, or 12 mM MgATP; in the presence or absence of 0.2 mM P_i. To bring the final volume to 120 μL, 16.7 μg of poly(C) or, for mock hydrolysis experiments, poly(dC), was added and a100 μL portion was immediately passed through a centrifuge column that had been preequilibrated in TKME buffer containing 0.5−10 mM MgATP. A sample (50 μL) of the 100 μL column eluate was taken for radioactivity measurement, as was 10 μL of the original mixture.

Nitrocellulose filter binding experiments were carried out as specified by Kim et al. (*23*) and also with modifications as described in the Results, using 24−25 mm filters from both Millipore, Inc. and Schleicher & Schuell, Inc.

Amicon Microcon-30 ultrafiltration devices were used as follows (G. Wang, personal communication): a portion (25 μL) of a 150 μL binding mixture containing Rho plus radiolabeled ligand was taken for determination of total radioactivity, and the remainder was placed above the membrane in the Microcon. The device was centrifuged at 5000*g* for 1 min, the filtrate (10−20 μL) was discarded, and the same device still containing sample above the membrane was placed in a fresh collection tube and was centrifuged again at 5000*g* for 6 min. A portion (25 μL) of the filtrate was subjected to liquid scintillation counting to determine the level of free ligand. This pre-spin protocol both removed residual glycerol from the Microcon membranes (which dilutes the sample that passes through) and saturated any adventitious ligand binding sites on the apparatus, each of which can confound the desired measurement (*22*).

Rapid mix/chemical quench experiments (*31*) were carried out as described (*22*).

RESULTS AND DISCUSSION

Three Nucleotide Binding Sites on Rho. Our previous ATP binding studies with Rho showed one class of three high-affinity sites per hexamer, $K_D = 0.2$ or 2 μM, depending on

[1] Abbreviations: ϵATP, 1,N^6-etheno-adenosine 5′-triphosphate.

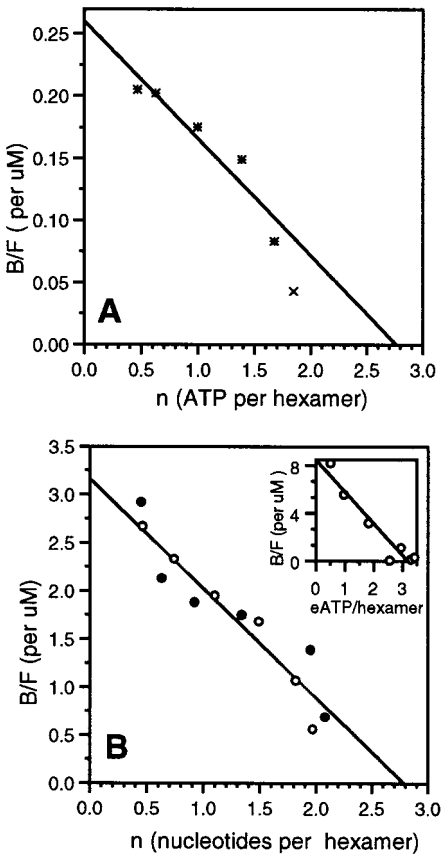

FIGURE 1: Adenine nucleotide binding to Rho. (A) Results of binding of [α-^{32}P]ATP to Rho with analysis by nitrocellulose filter binding (*23*). Samples were from 1 to 40 μM in [α-^{32}P]ATP at 1.2 $\times$ 10^4 cpm/nmol and contained 7.5 μg of Rho in a total of 20 μL. Two independent experiments using filters from different manufacturers are indicated (*, $\times$). n = 2.8 molecules of ATP per hexamer; K_D = 0.1 μM. (B) Comparison of binding of [γ-^{32}P]ATP (○) and [γ-^{32}P]ϵATP (●) to Rho with analysis by Microcon ultrafiltration (see Materials and Methods). Samples were from 0.5 to 2 μM in adenine nucleotide at (0.4−1.3) $\times$ 10^6 cpm/nmol and contained 8 μg of Rho, in TKME buffer with 5 mM potassium glutamate. n = 2.8 molecules of ATP per hexamer; K_D = 1.1 μM. (Inset) Results of a binding experiment using the same ϵATP as in panel B at from 1 to 30 μM and using 80 μg of Rho/sample, in TAGME buffer. n = 3.2 molecules of ϵATP per hexamer; K_D = 2.6 μM.

buffer conditions (*18*, *22*). Kim et al. (*23*), however, using nitrocellulose filters to measure ATP binding to Rho, reported three sites with K_D = 17 μM. We therefore carried out ATP binding experiments using the nitrocellulose filter technique. Figure 1 shows Scatchard plots indicating an ATP binding stoichiometry of 2.8 ATP molecules per Rho hexamer, K_D = 0.1 μM in 100 mM KCl buffer. When 150 mM potassium glutamate replaced KCl in the buffer, 2.5−3.2 ATP molecules/hexamer, K_D = 2−5 μM, were observed (data not shown). The data are in agreement with the nitrocellulose filter binding studies of Kim et al. (*23*) in number of sites, but, in agreement with our previous work (*18*) and that of Geiselmann and von Hippel (*19*), in KCl-containing buffer the K_D is 100-fold lower than that reported by Kim et al.

Binding studies were also conducted using ϵATP. In earlier work, fluorescence measurements indicated six ϵATP sites per Rho hexamer (*19*). However, using [γ-^{32}P]ϵATP and binding analysis by ultrafiltration, we again found three adenine nucleotide binding sites essentially identical in K_D to those for ATP (Figure 1B). Three ϵATP molecules per Rho hexamer were also found when higher protein and ligand concentrations were used (Figure 1B, inset). Our results continue to be consistent with the existence of three equivalent high-affinity adenine nucleotide binding sites on Rho.

No Hydrolysis Products Found Bound to Rho. Kim et al. (*23*) reported a class of "noncatalytic" ATP binding sites on Rho in which ATP is slowly hydrolyzed at 1.8 s^{-1} and products are released at only 0.02 s^{-1} as long as ATP hydrolysis continues in the 30 s^{-1} catalytic sites. These sites were observed in experiments in which Rho with RNA [poly(C)] was mixed with [α-^{32}P]ATP for <10 s, followed by the addition of excess unlabeled ATP and then assay of radioactivity bound to Rho by nitrocellulose filter binding. The concentration of [α-^{32}P]ATP was sufficiently high that it was not all consumed prior to addition of the unlabeled ATP. However, our attempts to replicate these results failed to detect radioactivity from [α-^{32}P]ATP reproducibly bound to the nitrocellulose when RNA was present (data not shown). Radioactivity in excess of background was reproducibly retained on the filters only in the absence of RNA, as in the ATP binding studies (Figure 1A). These results were unchanged by the use of nitrocellulose filters from different manufacturers, by variation in the length of preincubation of the filters in buffer, by prewashing the filters in NaOH, by omission of 10% glycerol from the buffer, by use of buffer with Mg^{2+} in 1 mM excess over the ATP present rather than at 10 mM, and by various rates of filtration. The results are consistent with retention of [α-^{32}P]-ATP by Rho on the nitrocellulose under nonhydrolysis conditions and with rapid hydrolysis and release of products from Rho in the presence of RNA.

We performed similar binding experiments using the alternative technique of centrifuge columns to separate bound from free nucleotides. A solution containing [^{3}H]ATP plus Rho was combined with poly(C) plus unlabeled ATP, and the mixture was immediately loaded onto a centrifuge column (see Materials and Methods). Less than 20 s elapsed between the start of mixing of the two solutions and the start of separation in the centrifuge; in this amount of time, according to our earlier rapid mix/chemical quench results (*22*), the labeled ATP initially bound to Rho should have been hydrolyzed at 30 s^{-1} and [^{3}H]ADP product released from Rho and retained in the column. Any [^{3}H]ADP hydrolysis product that is released at only 0.02 s^{-1}, however (*23*), should remain bound to Rho as it passes through the column. The column eluate was sampled for radioactivity. Only 0.6−1.6% of the radioactivity originally bound to Rho was recovered in the column eluate, consistent with hydrolysis and release, or direct release, of [^{3}H]ATP from the enzyme, and loss in the column. The results were similar when the centrifuge column was preequilibrated in buffer containing 10 mM unlabeled MgATP to ensure the presence of substrate throughout the experiment.

Centrifuge columns were also used to detect whether ADP could bind to Rho under hydrolysis conditions. Rho preincubated with unlabeled ATP plus [^{3}H]ADP was mixed with poly(C) and then immediately passed through a centrifuge column that had been preequilibrated with buffer containing unlabeled ATP. Negligible tritium was found in the column eluate. Similar results were found under mock hydrolysis conditions when poly(dC), which binds Rho similarly to

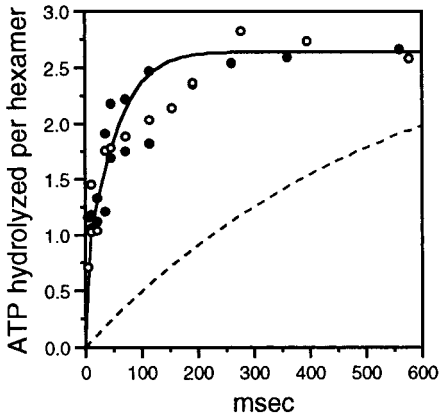

FIGURE 2: Results of two independent isotope partitioning experiments using the rapid mix/chemical quench apparatus. Rho at 1.8 mg/mL in TAGME buffer plus [γ-^{32}P]MgATP at 100 μM (36 000 cpm/nmol) was mixed with poly(C) RNA at 400 μg/mL plus nonradioactive MgATP at 8.5 mM; approximately 100 μL of mixed reagents was quenched after various times from 5 to 900 ms, and analyzed for ATP hydrolysis by measurement of product $^{32}P_i$ as described (*22*). The slow hydrolysis of [γ-^{32}P]ATP by Rho in the absence of RNA (*22*) was measured in each experiment and the appropriate amount of $^{32}P_i$ thus derived was subtracted from each point. (—) Simulation of expected results by KINSIM according to the author's model (see text); (- - -) simulation according to the model of Kim and Patel (*24*) (see text).

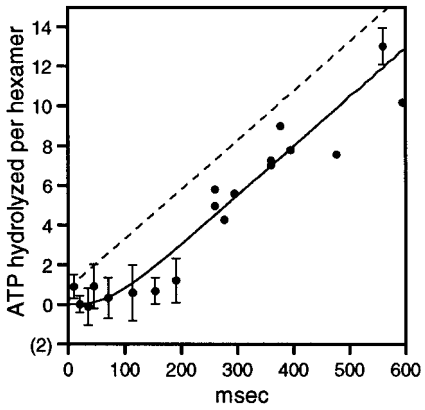

FIGURE 3: Results of five independent experiments in which Rho plus unlabeled ATP was mixed with RNA + excess [γ-^{32}P]ATP using the rapid mix/chemical quench apparatus; appearance of product $^{32}P_i$ was measured. Rho at 1.8 mg/mL in TAGME buffer plus MgATP at 40 or 80 μM was mixed with poly(C) RNA at 400 μg/mL plus labeled MgATP (2500−7500 cpm/nmol) at 0.5 or 1 mM, and samples were quenched after from 5 to 2100 ms. Hydrolysis plateaued starting at about 900 ms as the ATP was consumed. We estimate that in the rapid mix syringe that contained Rho plus unlabeled ATP, less than 10% of the ATP was hydrolyzed by Rho in the absence of RNA by the end of the experiment. This estimation was made using the hydrolysis rate measured in Stitt and Xu (*22*) and in experiments as described in the legend to Figure 2. The data were corrected for dilution of the labeled ATP by free unlabeled ATP upon mixing, assuming three filled ATP sites per Rho hexamer. (—) Simulation of expected results by KINSIM according to the author's model (see text); (- - -) simulation according to the model of Kim and Patel (*24*) (see text).

poly(C) but does not stimulate ATP hydrolysis (*32*), was used in place of poly(C). The inclusion of P_i in the enzyme mixture did not change the results.

In summary, using manual techniques, we were unable to detect ATP hydrolysis products bound to Rho during catalysis and could measure ATP bound to Rho only under non-hydrolysis conditions.

High-Affinity ATP Binding Sites of Rho Are Kinetically Competent. Previous experiments to ascertain the catalytic competence of the ATP binding sites of Rho were carried out by isotope partitioning experiments (*33*, *34*) that were conducted manually (*18*). In these experiments, Rho saturated with [γ-^{32}P]ATP was mixed with RNA plus a high concentration of nonradioactive ATP, and after various times the reaction was quenched with acid. Upon mixing with RNA plus unlabeled ATP, radioactive ATP bound to Rho is either hydrolyzed or dissociates from the protein and is diluted by the unlabeled ATP. Measurement of radiolabeled phosphate in the quenched reaction indicates the proportion of bound ATP that is hydrolyzed. The time resolution afforded by manual isotope partitioning experiments is not better than 0.5−1 s, however, and thus the kinetic competence of bound substrate molecules was not well determined. We therefore used rapid mix/chemical quench techniques to conduct isotope partitioning experiments with Rho, allowing determination of rate constants.

Figure 2 shows the results of isotope partitioning experiments in which Rho·[γ-^{32}P]ATP_3 is mixed with RNA plus a large excess of nonradioactive ATP, followed by acid quench of the reaction after various times as short as 5 ms. One molecule of [γ-^{32}P]ATP per Rho hexamer was found to be hydrolyzed at the earliest quench times (a burst of product formation), in agreement with previous results (*22*). Approximately 1.5 additional molecules of [γ-^{32}P]ATP have been hydrolyzed by 200 ms after mixing. These results indicate that all ATP molecules bound to Rho (Figure 1) are catalytically competent. The appearance of a burst of product suggests that the chemistry of ATP hydrolysis is rapid, and that a subsequent step in the catalytic cycle is rate determining (*31*).

Unlabeled ATP Molecules Bound to Rho Delay the Hydrolysis of Added [γ-^{32}P]ATP. The results of earlier rapid mix work (*22*) suggest that ATP molecules bound in the catalytic sites of Rho are hydrolyzed sequentially upon RNA binding. This interpretation specifically predicts that when Rho saturated with unlabeled ATP is mixed with RNA plus excess [γ-^{32}P]ATP, there will be a lag in the appearance of product $^{32}P_i$ while the bound, unlabeled ATP molecules are hydrolyzed: the first [γ-^{32}P]ATP molecule hydrolyzed will be the fourth ATP molecule consumed by that enzyme molecule. Figure 3 shows the results of such experiments: a lag in the appearance of product $^{32}P_i$ of at least 100 ms is seen, followed by steady-state hydrolysis of labeled ATP.

Kinetic Modeling. The data in Figures 2 and 3 have been simulated (solid lines) using KINSIM (*35*) with a single model having the following properties. Rho has three catalytic sites in which ATP binds. RNA then associates with Rho·ATP_3 and causes rapid hydrolysis (300 s^{-1}) of one molecule of ATP per hexamer (the burst). The occurrence of chemistry is followed by a rate-limiting step (product release or an enzyme conformation change) at 27 s^{-1}. Additional bound ATP molecules, in fixed order around the hexamer, undergo similar net hydrolysis at 27 s^{-1} (chemistry at 300 s^{-1} plus a 27 s^{-1} slow step) or can at any time dissociate from Rho at 2 s^{-1}. There is good agreement between this model and the data.

The effects on the model of changes in the rates were examined. Altering the rate at which chemistry occurs has

Scheme 1

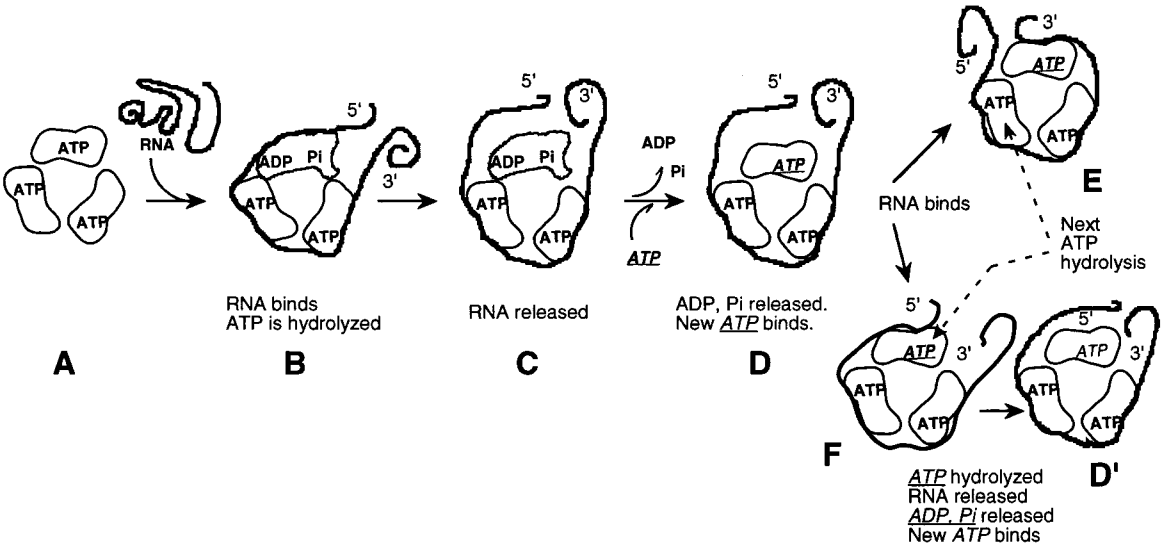

the greatest effect on the size of the ATP hydrolysis burst (Figure 2). Rates of 250 s^{-1} or faster are consistent with the data; at 200 s^{-1}, only 0.6 molecule of ATP would be hydrolyzed per hexamer at 5 ms, a difference that would have been seen experimentally. Variations in the value of k_{off} for ATP also have the largest effect on isotope partitioning experiments (Figure 2). Lower values result in hydrolysis of a greater proportion of initially bound [γ-^{32}P]ATP molecules. The maximal number of [γ-^{32}P]ATP molecules hydrolyzed was ~2.6/hexamer (Figure 2), well-fit by an off-rate of 2 s^{-1}. Although 7 s^{-1} was the dissociation rate calculated from the measured K_D value for ATP from Rho using k_{cat}/K_M as a minimal value for k_{on} (*22*), this off-rate predicted hydrolysis of only 2.25 [γ-^{32}P]ATP molecules per hexamer. These results thus suggest that the ATP dissociation rate from Rho·RNA·ATP complexes may be slightly slower than from Rho·ATP complexes. Finally, the rate of the slow step in the catalytic cycle affects chiefly the fit of the model to the steady-state portion of curves in Figure 3, but lower values also slightly increase the lag. Values between 25 and 30 s^{-1} best fit the steady-state data obtained.

The data in Figure 3 suggest a longer lag than is predicted by the KINSIM models. However, we suspect that points between 100 and 200 ms may be artifactually low. For the rapid mix conditions used to obtain these points, calculation of a Reynolds number (*31*) yielded a value less than 2000, indicating that turbulent mixing of the reactants may not have occurred. Inadequate mixing could result in lower hydrolysis of the labeled [γ-^{32}P]ATP, which in turn means that the lag may be shorter than indicated by our results.

An Alternative Model Does Not Fit the Present Data. Kim et al. (*23*) and Kim and Patel (*24*) propose a model for Rho in which the three sites per hexamer that can catalyze ATP hydrolysis at 30 s^{-1} at 18 °C also readily exchange ATP. These catalytic sites are termed "loose" ATP binding sites, and are not detected in ATP binding experiments. The three sites in which ATP binding to Rho is detectable were termed "tight" sites; upon RNA binding they are proposed to hydrolyze ATP molecules independently of one another at 1.8 s^{-1} at 18 °C while, concurrently, the "loose" sites hydrolyze ATP molecules sequentially at 30 s^{-1}. Due to their slow ATP hydrolysis rate relative to the catalytic sites, these sites have been termed "noncatalytic". Simulation of this model by KINSIM for an isotope partitioning experiment yields slow hydrolysis of the three labeled ATP molecules that are tightly bound to Rho (Figure 2, dashed line). In an experiment like that in Figure 3, when unlabeled ATP is prebound to Rho and chased with [γ-^{32}P]ATP, this model predicts no delay in the appearance of $^{32}P_i$ product. Labeled ATP binds rapidly from the medium to the catalytic sites, and assuming, as above, chemistry at 300 s^{-1} followed by a 27 s^{-1} slow step, the dashed line in Figure 3 shows the expected appearance of product $^{32}P_i$. There is a burst of one ATP molecule per hexamer followed immediately by steady-state hydrolysis. This model is clearly not compatible with the data presented in Figures 2 and 3.

Model for Rho Function. The results of the experiments presented here support the presence of three high-affinity binding sites for ATP per Rho hexamer, all of which are catalytic sites, and in which previously bound ATP molecules are hydrolyzed sequentially at 30 s^{-1} at 21 °C upon RNA binding. An overall model for ATP hydrolysis by Rho coupled with 5′ → 3′ travel by the enzyme along RNA is depicted in Scheme 1; this model is similar to one proposed by Geiselmann et al. (*36*). Rho is drawn as a trimer of dimers (A). The trigger for ATP hydrolysis in this model is interaction of RNA with a free 5′ region to a Rho active unit that has ATP bound (B, E, and F). The free 5′ region makes possible Rho-RNA configurations that are not available to the other Rho active units, and that trigger ATP hydrolysis. ATP hydrolysis causes complete RNA release from this site (C, D′), and following the dissociation of hydrolysis products and binding of a new ATP molecule from the medium (D, D′), RNA can again bind. Scheme 1 shows that two different portions of the long RNA molecule bound to Rho might compete for this binding. If a more 3′ RNA region binds (E), Rho achieves travel along the RNA and the next Rho active unit, which now is associated with RNA with a free 5′ region, is triggered to hydrolyze its bound ATP molecule. If the same region of RNA that was just released rebinds (F), the same active unit that just catalyzed hydrolysis will fruitlessly hydrolyze a second molecule of ATP, without associated movement of Rho with respect to RNA (F, D′). The results of the experiments of Figure 3 indicate that the

latter possibility occurs rarely; sequential hydrolysis of all three ATP molecules intially bound is the norm, with a consequent delay in hydrolysis of the first ATP molecule that binds from the medium. A conformation change in Rho upon the release of RNA, ADP, or Pi might prevent such RNA rebinding. Various paths for an RNA molecule among the Rho subunits, other than the simple one depicted, could be compatible with this model.

The model in Scheme 1 predicts that the stoichiometry of ATP hydrolysis as Rho moves along RNA would be 1 ATP molecule/∼25 bases, the length of RNA bound to one Rho dimer. This prediction is at variance with the existing measurements of 1−2 and 40 ATP molecules hydrolyzed per base of RNA, which were made using natural messages (*3*, *37*). The present model is based on experiments using poly(C); further work with natural RNAs may clarify this issue.

The model in Scheme 1 is not readily compatible with tethered tracking models that have been proposed for Rho (*38*, *39*). In tethered tracking, Rho retains one segment of RNA in some of its binding sites while successively more 3′ regions of the same RNA molecule are bound and released in other sites as ATP is hydrolyzed. Evidence in support of tethered tracking has been alternatively interpreted as the result of either rapid rebinding of released Rho to RNA (*38*) or of cooperative binding of more than one Rho hexamer at a particular RNA location (*3*).

The present results indicate that ATP binding, hydrolysis, and release of hydrolysis products by one class of Rho site is responsible for changes in Rho interactions with RNA. The sequential hydrolysis pattern is compatible with simple tracking by Rho 5′ → 3′ along RNA (Scheme 1; refs *3* and *36*).

ACKNOWLEDGMENT

We would like to thank C. Grubmeyer for use of the rapid mix/chemical quench apparatus, for valuable discussions, and for reading the manuscript.

REFERENCES

1. Richardson, J. P., and Greenblatt, J. (1996) in *Escherichia coli and Salmonella* (Neidhardt, F. C., et al., Eds.) pp 822−848, ASM Press, Washington, DC.
2. Brennan, C. A., Dombroski, A. J., and Platt, T. (1987) *Cell 48*, 945−952.
3. Walstrom, K. M., Dozono, J. M., and von Hippel, P. H. (1997) *Biochemistry 36*, 7993−8004.
4. Gogol, E. P., Seifried, S. E., and von Hippel, P. H. (1991) *J. Mol. Biol. 221*, 1127−1138.
5. Horiguchi, T., Miwa, Y., and Shigesada, K. (1997) *J. Mol. Biol. 269*, 514−528.
6. Egelman, E. H., Yu, X., Wild, R., Hingorani, M. M., and Patel, S. S. (1995) *Proc. Natl. Acad. Sci. U.S.A. 92*, 3869−3873.
7. Walker, J. E., Saraste, M., Runswick. M. J., and Gay, N. J. (1982) *EMBO J. 1*, 945−951.
8. Allison, T. J., Wood, T. C., Briercheck, D. M., Rastinejad, F., Richardson, J. P., and Rule, G. S. (1998) *Nat. Struct. Biol. 5*, 352−356.
9. Briercheck, D. M., Wood, T. C., Allison, T. J., Richardson, J. P., and Rule, G. S. (1998) *Nat. Struct. Biol. 5*, 393−399.
10. Bogden, C. E., Fass, D., Bergman, N., Nichols, M. D., and Berger, J. M. (1999) *Mol. Cell 3*, 487−493.
11. Dombroski, A. J., and Platt, T. (1988) *Proc. Natl. Acad. Sci. U.S.A. 85*, 2538−2542.
12. Opperman, T., and Richardson, J. P. (1994) *J. Bacteriol. 176*, 5033−5043.
13. Miwa, Y., Horiguchi, T., and Shigesada, K. (1995) *J. Mol. Biol. 254*, 815−837.
14. Boyer, P. D. (1997) *Annu. Rev. Biochem. 66*, 717−749.
15. Magyar, A., Zhang, X., Abdi, F., Kohn, H., and Widger, W. R. (1999) *J. Biol. Chem. 274*, 7316−7324.
16. Vincent, F., Openshaw, M., Trautwein, M., Gaskell, S. J., Kohn, H., and Widger, W. R. (2000) *Biochemistry 39*, 9077−9083.
17. Yu, X., Horiguchi, T., Shigesada, K., and Egelman, E. H. (2000) *J. Mol. Biol. 299*, 1279−1287.
18. Stitt, B. L. (1988) *J. Biol. Chem. 263*, 11130−11137.
19. Geiselmann, J., and von Hippel, P. H. (1992) *Protein Sci. 1*, 850−860.
20. Wang, Y., and von Hippel, P. H. (1993) *J. Biol. Chem. 268*, 13947−13955.
21. Seifried, S. E., Bjornson, K. P., and von Hippel, P. H. (1991) *J. Mol. Biol. 221*, 1139−1151.
22. Stitt, B. L., and Xu, Y. (1998) *J. Biol. Chem. 273*, 26477−26486.
23. Kim, D.-E., Shigesada, K., and Patel, S. S. (1999) *J. Biol. Chem. 274*, 11623−11628.
24. Kim, D.-E., and Patel, S. S. (1999) *J. Biol. Chem. 274*, 32667−32671.
25. Mott, J. E., Grant, R. A., Ho, Y.-S., and Platt, T. (1985) *Proc. Natl. Acad. Sci. U.S.A. 82*, 88−92.
26. Nehrke, K. W., Seifried, S. E., and Platt, T. (1992) *Nucleic Acids Res. 20*, 6107.
27. Geiselmann, J., Yager, T. D., Gill, S. C., Calmettes, P., and von Hippel, P. H. (1992) *Biochemistry 31*, 111−121.
28. Glynn, I. M., and Chappell, J. B. (1964) *Biochem. J. 90*, 147−149.
29. Grubmeyer, C., and Penefsky, H. S. (1981) *J. Biol. Chem. 256*, 3718−3727.
30. Penefsky, H. S. (1977) *J. Biol. Chem. 252*, 2891−2899.
31. Johnson, K. A. (1995) *Methods Enzymol. 249*, 38−61.
32. Richardson, J. P. (1982) *J. Biol. Chem. 257*, 5760−5766.
33. Rose, I. A. (1980) *Methods Enzymol. 64*, 47−59.
34. Rose, I. A. (1995) *Methods Enzymol. 249*, 315−340.
35. Barshop, B. A., Wrenn, R. F., and Frieden, C. (1983) *Anal. Biochem. 130*, 134−145.
36. Geiselmann, J., Wang, Y., Seifried, S. E., and von Hippel, P. H. (1993) *Proc. Natl. Acad. Sci. U.S.A. 90*, 7754−7758.
37. Brennan, C. A., Steinmetz, E. J., Spear, P., and Platt, T. (1990) *J. Biol. Chem. 265*, 5440−5447.
38. Faus, I., and Richardson, J. P. (1990) *J. Mol. Biol. 212*, 53−66.
39. Steinmetz, E. J., and Platt, T. (1994) *Proc. Natl. Acad. Sci. U.S.A. 91*, 1401−1405.

BI002253A